The role of Mie scattering in the seeding of matter-wave superradiance

Romain Bachelard, Helmar Bender, Philippe W. Courteille, Nicola Piovella, Christian Stehle, Claus Zimmermann, Sebastian Slama

The role of Mie scattering in the seeding of matter-wave superradiance

R. Bachelard[a], H. Bender[a,c], and Ph.W. Courteille[a]
[a] *Instituto de Física de São Carlos, Universidade de São Paulo, 13560-970 São Carlos, SP, Brazil*

N. Piovella[b]
[b] *Dipartimento di Fisica, Università Degli Studi di Milano and INFM,Via Celoria 16, I-20133 Milano, Italy*

C. Stehle[c], C. Zimmermann[c], and S. Slama[c]
[c] *Physikalisches Institut, Eberhardt-Karls-Universität Tübingen, D-72076 Tübingen, Germany*
(Dated: May 29, 2012)

Matter-wave superradiance is based on the interplay between ultracold atoms coherently organized in momentum space and a backscattered wave. Here, we show that this mechanism may be triggered by Mie scattering from the atomic cloud. We show that the system evolves into a superposition of states, where the scattering process imprints a *phase grating* on the atomic dipoles. This grating generates coherent emission even when there is at most one excited atom in the system at a time, contributing to the backward light wave onset. The atomic recoil 'halos' created by the scattered light exhibit a strong anisotropy, in contrast to single-atom scattering.

PACS numbers: 42.50.Ct, 03.75.-b, 42.50.Gy

Matter wave superradiance (MWSR) [1] and collective atomic recoil lasing (CARL) [2, 3] are light-induced instabilities of the density distribution in atomic clouds. More precisely, they are due to correlations between successive scattering events mediated by long-lived coherences in the motional state of an (ultracold) atomic cloud or in the light field of an optical resonator [4]. Despite considerable theoretical efforts having been devoted to the dynamics of MWSR [5–7], open questions still remain. One of them concerns the seeding mechanism which is able to start the MWSR instability also in the presence of losses. Thermal and quantum fluctuations are natural candidates, however, in this paper we point out the particular role of Mie scattering which turns out to be important at the onset of MWSR. Being active before any instability has developed, it induces a *phase* correlation between the atomic dipoles which favors the build up of an instability.

The below-threshold dynamics and the seeding of matter-wave superradiance are interesting problems. As long as we consider the atomic cloud as a homogeneous entity, e.g. a Bose-Einstein condensate (BEC) in the mean field description, no scattering should occur at all. Theoretical models which describe BECs as matter waves without fluctuations thus fail to explain how MWSR starts when no seeding wave is present [8]. On the other hand, recent work has shown [9, 10] how atomic coarse-graining, density fluctuations and Mie scattering from finite-sized clouds can influence the scattering even of a single photon. Also optical cavities may strongly affect the scattering by shaping the angular distribution of the density of modes that are capable of receiving the scattered photons [11, 12]. These processes have a decisive impact on the mode competition preceding the exponential instability, and hence on the instability itself.

Here we show,that Mie scattering, caused by the finite size of the atomic cloud, favors the formation of a matter wave dipole grating. This has already been suspected in [13]. Indeed, prior to any significant motion of the atoms, their dipoles collectively order which in turn leads to coherent emission.

In previous papers [14–17], we discussed the impact of atomic coarse-graining and finite scattering volumes on the radiation pressure force which acts on the cloud's center-of-mass. Here, we investigate the momentum distribution after a cooperative single-photon scattering process from a BEC. Our theoretical model describes the atomic cloud as a macroscopic matter wave which is homogeneously distributed within a sphere, i.e. the atoms are considered to be strongly delocalized and density fluctuations are neglected. We find that the momentum distribution of the atoms adopts the shape of a *recoil halo*, very similar to the ones observed experimentally in time-of-flight images of BECs. The halo indicates the directions into which the atoms are preferentially scattered *before* the density distribution is noticeably modified. In particular, it exhibits a pronounced peak at $2\hbar k$. This corresponds to an increased backscattering of light, that acts as a seed for MWSR.

The atomic cloud is described as a bosonic ensemble of N two-level atoms with field operator $\hat{\Psi}(\mathbf{r},t) = \hat{\Psi}_g(\mathbf{r},t) + \hat{\Psi}_e(\mathbf{r},t)$ (g for the ground state, e for the excited one). We treat the condensate as an ideal gas and consider the scattering between matter wave and optical waves, but neglect nonlinearities due to atom-atom interaction. In second quantization, the interaction between the atoms

and light is described by the Hamiltonian [14, 18]

$$\hat{H}(t) = \frac{\hbar\Omega_0}{2}\int d\mathbf{r}\left[\hat{\Psi}_e^\dagger(\mathbf{r},t)\hat{\Psi}_g(\mathbf{r},t)e^{-i\Delta_0 t+i\mathbf{k}_0\cdot\mathbf{r}}+h.c.\right] \quad (1)$$
$$+\hbar\sum_{\mathbf{k}} g_{\mathbf{k}}\int d\mathbf{r}\left[\hat{\Psi}_e^\dagger(\mathbf{r},t)\hat{\Psi}_g(\mathbf{r},t)\hat{a}_{\mathbf{k}}e^{-i\Delta_k t+i\mathbf{k}\cdot\mathbf{r}}+h.c.\right],$$

where the first (second) line describes the absorption and emission of a pump mode Ω_0 (a vacuum mode $\hat{a}_{\mathbf{k}}$). Doppler effects are neglected. Replacing $\hat{\Psi}_e(\mathbf{r},t) \to \hat{\Psi}_e(\mathbf{r},t)e^{i\Delta_0 t}$ induces an energy shift of $-\Delta_0|\hat{\Psi}_e|^2$ in the Hamiltonian from which the Heisenberg equations may be derived:

$$\frac{\partial\hat{\Psi}_g}{\partial t} = -i\hat{\Psi}_e\left[\frac{\Omega_0}{2}e^{-i\mathbf{k}_0\cdot\mathbf{r}}+\sum_{\mathbf{k}} g_{\mathbf{k}}\hat{a}_{\mathbf{k}}^\dagger e^{-i(\Delta_0-\Delta_k)t-i\mathbf{k}\cdot\mathbf{r}}\right] \quad (2)$$

$$\frac{\partial\hat{\Psi}_e}{\partial t} = -i\hat{\Psi}_g\left[\frac{\Omega_0}{2}e^{i\mathbf{k}_0\cdot\mathbf{r}}+\sum_{\mathbf{k}} g_{\mathbf{k}}\hat{a}_{\mathbf{k}}e^{i(\Delta_0-\Delta_k)t+i\mathbf{k}\cdot\mathbf{r}}\right] + i\Delta_0\hat{\Psi}_e \quad (3)$$

$$\frac{\mathrm{d}\hat{a}_{\mathbf{k}}}{\mathrm{d}t} = -ig_{\mathbf{k}}e^{-i(\Delta_0-\Delta_k)t}\int d\mathbf{r}\hat{\Psi}_g^\dagger(\mathbf{r},t)\hat{\Psi}_e(\mathbf{r},t)e^{-i\mathbf{k}\cdot\mathbf{r}}. \quad (4)$$

For large atom numbers and for far detuning from the atomic transition frequency, one can neglect quantum fluctuations and treat the operators as c-numbers ($\hat{\Psi} \to \psi$). Eq.(4) is integrated over time as

$$a_{\mathbf{k}} = -ig_{\mathbf{k}}\int_0^t \mathrm{d}t' e^{-i(\Delta_0-\Delta_k)t'}\int d\mathbf{r}\psi_g^*(\mathbf{r},t')\psi_e'(\mathbf{r},t)e^{-i\mathbf{k}\cdot\mathbf{r}}, \quad (5)$$

and inserted into (3). Furthermore, we switch to a continuous-mode description $\sum_{\mathbf{k}} \to (V_\nu/(2\pi)^3)\int \mathrm{d}\mathbf{k}$ and obtain:

$$\frac{\partial\psi_e}{\partial t} = i\Delta_0\psi_e(\mathbf{r},t) - i\frac{\Omega_0}{2}e^{i\mathbf{k}_0\cdot\mathbf{r}}\psi_g(\mathbf{r},t) - \psi_g(\mathbf{r},t)\int \mathrm{d}\mathbf{r}' \quad (6)$$
$$\times\int \mathrm{d}\mathbf{k} g_{\mathbf{k}}^2 e^{i\mathbf{k}\cdot(\mathbf{r}-\mathbf{r}')}\int_0^t \mathrm{d}t' e^{i(\Delta_0-\Delta_k)(t-t')}\psi_g^*(\mathbf{r}',t)\psi_e(\mathbf{r}',t').$$

During the short time of the incident light pulse, the atomic density does not significantly change, i.e. $\psi_g(\mathbf{r},t) \approx \psi_{g0}(\mathbf{r})$ in (6) with $\rho_0(\mathbf{r}) = |\psi_{g0}(\mathbf{r})|^2$ being the initial density of the cloud. Using the Markov approximation, i.e. the photon time of flight through the cloud is much shorter than the atomic decay time, the last integral in (6) is replaced by $\delta(k-k_0)\psi_{g0}(\mathbf{r}')\psi_e(\mathbf{r}',t)/c$. With the assumption that all the electromagnetic modes are equally present in the system ($g_{\mathbf{k}} \approx g_{k_0}$) and by keeping rotating-wave-approximation terms, one can show that [19]:

$$\int \mathrm{d}\mathbf{k} g_{\mathbf{k}}^2 e^{i\mathbf{k}\cdot\mathbf{d}}\int_0^\infty \mathrm{d}t' e^{i(\Delta_0-\Delta_k)(t-t')} = \frac{\Gamma}{2ik_0|\mathbf{d}|}e^{ik_0|\mathbf{d}|}, \quad (7)$$

where $\Gamma = V_\nu g_{k_0}^2 k_0^2/\pi c$ is the atomic decay rate. For the normalized excitation field $\beta(\mathbf{r},t) = \psi_e(\mathbf{r},t)/\psi_{g0}(\mathbf{r})$ with $|\beta(\mathbf{r})|^2$ being the probability for an atom to be excited, one obtains [25]

$$\frac{\partial\beta(\mathbf{r},t)}{\partial t} = \left(i\Delta_0-\frac{\Gamma}{2}\right)\beta(\mathbf{r},t) - i\frac{\Omega_0}{2}e^{i\mathbf{k}_0\cdot\mathbf{r}}$$
$$-\frac{\Gamma}{2}\int \mathrm{d}\mathbf{r}'\rho_0(\mathbf{r}')\frac{\exp(ik_0|\mathbf{r}-\mathbf{r}'|)}{ik_0|\mathbf{r}-\mathbf{r}'|}\beta(\mathbf{r}',t). \quad (8)$$

which recovers the model of cooperative scattering of a plane-wave introduced in [14].

Eq.(8) can be used to describe the scattering of light from a dielectric medium with an index of refraction $m_c = \sqrt{1-4\pi\rho_0\Gamma/k_0^3(\Delta_0+i\Gamma/2)}$ in the steady-state regime [17]. The excitation pattern inside the cloud can be calculated analogous to Mie's theory [20, 21]: the electromagnetic fields inside and outside the cloud are decomposed into elementary solutions of the Helmholtz equation $(\Delta+m_c^2k_0^2)\beta = 0$ and their amplitudes are calculated according to the boundary conditions on the fields. For a homogeneous spherical cloud of radius R, the field $\beta(\mathbf{r})$ reads:

$$\beta(\mathbf{r}) = \frac{dE_0}{\hbar\Gamma}\sum_{n=0}^{\infty}(2n+1)i^n\beta_n j_n(m_c k_0 r)P_n(\cos\theta), \quad (9)$$

with j_n the spherical Bessel functions and P_n the Legendre polynomials (see e.g. [17] for an expression of the scattering coefficients β_n). Note, that the excitation field β satisfies the Helmholtz equation. This means that Mie scattering actually imprints a *phase grating* (with wavevector $m_c k_0$) onto the wavefunction of the excited state. This phase grating will be at the origin of the backscattering wave that acts as a seed for MWSR. Indeed, the field radiated by the atoms inside the cloud in a direction $\mathbf{u}(\theta,\phi)$ is given by the structure factor:

$$s_c(\mathbf{u}) = \frac{1}{N}\int \rho(\mathbf{r})\beta(\mathbf{r})e^{-im_c k_0\mathbf{u}\cdot\mathbf{r}}\mathrm{d}\mathbf{r}, \quad (10)$$

with the index of refraction m_c given above. Hence, the coherent emission by the cloud is a direct consequence of periodic excitation field and the resulting dipole grating.

The scattered light is difficult to observe directly, however, the radiation pattern is also present in the momentum distribution of the atoms which can be easily recorded by time of flight imaging. Different to an N-body model, the quantum matter field approach yields the momentum distribution simply as the Fourier transform of the matter field, $\widehat{\psi}(\mathbf{p}) = (2\pi\hbar)^{-3}\int\psi(\mathbf{r})e^{-i\mathbf{p}\cdot\mathbf{r}/\hbar}\mathrm{d}\mathbf{r}$. Hence, for an homogeneous cloud, the momentum distribution of the excited state is directly proportional to the structure factor: $\widehat{\psi}_e(\mathbf{p}) \propto s_c(\mathbf{p}/\hbar)$, with $\mathbf{p} = m_c\hbar\mathbf{k}$ and $\mathbf{k} = k_0\mathbf{u}$. Using Eq.(9), it can be deduced that the momentum wavefunction $\widehat{\psi}_e$ for an uniform sphere of radius R reads:

$$\widehat{\psi}_e(\mathbf{p}) = \frac{dE_0\sqrt{\rho_0}}{\hbar\Gamma(2\pi\hbar)^3}\sum_{n=0}^{\infty}(2n+1)\beta_n\gamma_n(p)P_n(\cos\theta), \quad (11)$$

with $\gamma_n(p) = 4\pi \int_0^R r^2 j_n(m_c k_0 r) j_n(pr/\hbar)\mathrm{d}r$. Fig.1(a)

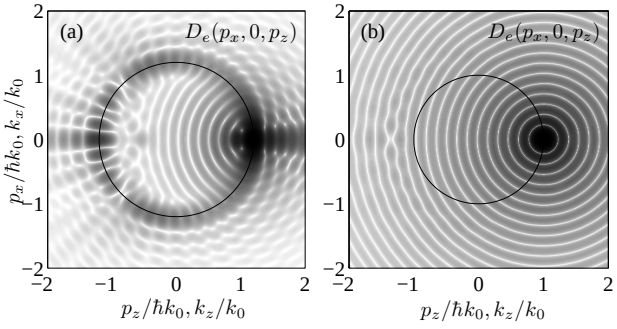

FIG. 1. Momentum distribution of the excited state $D_e = |\widehat{\psi}_e|^2$, in logarithmic scale. The emission pattern $|s_c(\mathbf{k})|^2$ concentrates around a circle with radius $p = m_c\hbar k_0$ (black line). Simulations for a laser detuning $\Delta_0 = -3$GHz and a cloud (a) of size $k_0 R = 20$, atom number $N = 1.15 \times 10^6$ and refractive index $m_c = 1.2$, (b) of size $k_0 R = 20$, atom number $N = 1$ and refractive index $m_c = 1 + 2.10^{-7}$. For rubidium, $k_0^{Rb} = 8.05 \times 10^6 \mathrm{m}^{-1}$ and $\Gamma^{Rb} = 6.1$MHz.

shows a typical momentum distribution of the excited atoms $|\widehat{\psi}_e(\mathbf{p})|^2$ and the associated scattering pattern $|s_c(\mathbf{k})|^2$ of the light. Different to a single-atom process, Mie scattering turns out to be fundamentally anisotropic. The matter field allows for multiple scattering i.e. an atom may absorb a photon that was already scattered. This explains the presence of a halo for the excited state. In optically dilute clouds multiple scattering is reduced with the consequence of less pronounced halos. For large clouds ($k_0 R \gg 1$), most of the photons are scattered into the forward direction, a process that leaves the atomic momentum distribution unchanged. For example, in Fig.1(a), most atoms recoil to $\mathbf{k} = k_0 \hat{z}$. Nevertheless, a significant amount of light is still scattered backward ($\mathbf{k} = -k_0 \hat{z}$) and acts as a seed for the MWSR instability.

Note that the momentum distribution $D_e(\mathbf{p}) = |\widehat{\psi}_e(\mathbf{p})|^2$ is concentrated along a circle with radius $p = m_c\hbar k_0$ rather than $\hbar k_0$ (i.e. that $\gamma_n(p)$ reaches a maximum for $p = m_c\hbar k_0$) . This is a signature of the Minkowski momentum for atomic recoil [22]. The blurring of the momentum wavefunction along the circle originates in the finite size of the cloud, that creates a natural momentum spread $\sigma_p \sim \hbar/R$. The ripples of the distribution are due to the sharp boundary of the cloud's density, yielding a Fourier transform with many secondary peaks.

The halo shown in Fig.1(a) and its radius of $m_c\hbar k_0$ instead of $\hbar k_0$ is a clear indication that a single photon is scattered by all atoms collectively [15], since multiple scattering now allows for absorption of photons nonparallel to the laser. For comparison, the excited state momentum distribution for a single atom is shown in Fig.1(b) ($N = 1$). As expected, Rayleigh scattering from individual, initially delocalized atom does not exhibit the intricate pattern of Mie scattering and the momentum distribution is simply centered at $\hbar k_0$. If the atoms are initially localized, e.g. for non-condensed clouds of atoms, the momentum distribution enlarges and the halo washes out eventually. Note that our model neglects the single-atom isotropic decay pattern, that yields a uniform halo, so that it is not valid at very low density.

After an atom absorbs a photon from the laser with a momentum kick $m_c\hbar\mathbf{k}_0$ the photon is reemited according to the Mie pattern $s_c(\mathbf{p}/\hbar) \propto \widehat{\psi}_e(\mathbf{p})$. Thus the atom will gain an extra momentum $m_c\hbar k_0$ with a direction opposite to the emitted photon and the momentum pattern of the ground state atoms after the scattering process is given by $|\widehat{\psi}_e(m_c\hbar\mathbf{k}_0 - \mathbf{p})|^2$. Experimentally, the *column-integrated* momentum distribution is observed in time of flight images. This leads to defining the projected distribution $D_g^y(p_x, p_z) = \int |\hat{\psi}_g(\mathbf{p})|^2 \mathrm{d}p_y$. Such an integrated distribution is presented in Fig.2(a). The atoms are observed to *inhomogeneously* fill a circle of radius $m_c\hbar k_0$. In particular, the part of the sphere around $\mathbf{p} = (3/2)\hbar\mathbf{k}_0$ is weakly populated, which reflects the anisotropic nature of Mie scattering.

Experimentally, the atomic recoil patterns are investigated by using the set-up of [10]. After the interaction with the light, the ^{87}Rb atoms ballistically expand for $t_F = 20ms$. The density distribution of the expanded cloud is recorded by standard absorption imaging yielding the initial momentum distribution before the expansion according to $\mathbf{p} = m_{Rb}\mathbf{r}/t_F$ (the initial size of the cloud $\sim 20\mu m$ is much smaller than its expanded size at the time of imaging).

The integrated momentum distribution observed experimentally reproduces the features predicted by Mie scattering (see Fig.2(b)). A sphere of radius $\hbar k_0$ is filled with atoms, yet it exhibits a region where the probability of the atomic recoil is very low around $p_z = 1.5\hbar k_0$. Moreover, it can be observed that a large number of atoms recoil around the $\mathbf{p} = 2\hbar\mathbf{k}_0$, that are the signature of the backward emitted wave. This is opposite to single-atom scattering that scatter photons in random directions, and not particularly backward and forward.

It is important to note that Mie scattering is a three-dimensional process, while the MWSR only develops along its most unstable direction. Mie scattering is a seeding process that sends photons in many directions, particularly also backwards, which is known to be the most unstable direction for MWSR in a cigar-shaped cloud illuminated along its main axis.

These two processes are illustrated in Fig.3. Initially, Mie scattering populates a sphere of radius $p \approx m_c\hbar k_0$. Then a MWSR instability develops, i.e. the phase grating induces light emission that, in turn, starts amplifying this atomic grating. The atoms observed in $\mathbf{p} \approx -2m_c\hbar\mathbf{k}_0$ and $\mathbf{p} \approx 4m_c\hbar\mathbf{k}_0$ are not predicted by Mie scattering and can be explained only by the self-consistent matter-wave dynamics.

In this paper we showed that Mie scattering induces a

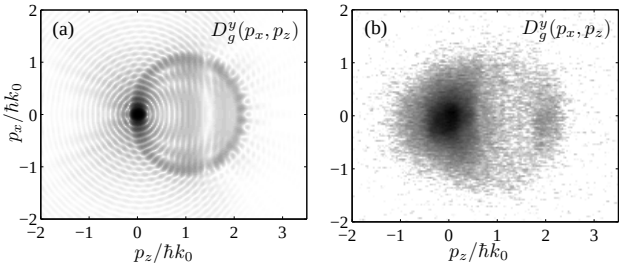

FIG. 2. (a) Integrated momentum distribution of the excited state, calculated from Eq.11 for a spherical homogeneous cloud of radius $k_0R = 29.6$, $\Delta_0 = -15$GHz and with a refractive index $m_c = 1.067$ (a low-pass Gaussian filter was applied to attenuate the ripples due to the sharp boundaries of the homogeneous clouds, since they are irrelevant for comparison with the experiment) (b) Experimental integrated momentum distribution of the ground state for an ellipsoidal cloud of length $k_0\sigma_z \sim 29.6$, transverse radius $k_0\sigma_\perp \sim 4.7$, with $N \sim 147000$ atoms and a laser detuning $\Delta_0 = -15$GHz and a $20\mu s$ laser pulse of 17mW. Its refractive index is $m_c \approx 1.067$.

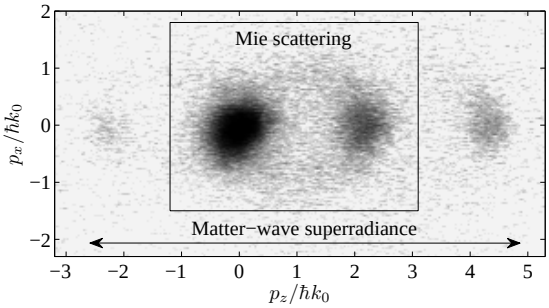

FIG. 3. Momentum distribution $|\widehat{\psi_g}|^2$ *above* the threshold of the MWSR. Experiment realized with an ellipsoidal cloud of transverse radius $k_0\sigma_\perp \sim 3.5$, length $k_0\sigma_z \sim 22$, with $N \sim 156000$ atoms and a laser detuning $\Delta_0 = -15$GHz.

grating in the atomic dipole distribution even below the threshold for the MWSR instability. Its signature is an anisotropic three-dimensional halo in the of atomic momentum distribution. The atoms observed at $\mathbf{p} \approx 2\hbar\mathbf{k}_0$ generate a seeding wave for MWSR. Indeed, the matter wave modes at 0 and $2\hbar\mathbf{k}_0$ together form density grating at which subsequent photons injected from the pump laser are Bragg-scatterered in a self-amplifying process.

Note that a mean-field approach such as the Timed-Dicke State [23] does not yield any halo: the Fourier transform of a $\beta_{TDS}e^{-i\mathbf{k}_0.\mathbf{r}}$ state will lead to a Dirac function in momentum space, up to the finite size of the cloud, and the absorption-reemission process $\psi_e\psi_e^*$ will automatically send back the atoms in $\mathbf{p} \approx \mathbf{0}$. Thus, a three-dimensional approach such as the Mie theory is required to describe the observed anisotropic halos.

Finally, it is interesting to remark that the off-axis emission of photons should be associated to higher modes ($n \gg 1$) that correspond to photons with long lifetime within the cloud [24]. Thus, a time-resolved observation of the off-axis atomic recoils should bear the signature of subradiance.

We acknowledge helpful discussion with R. Kaiser. This work has been supported by the Fundação de Amparo Pesquisa do Estado de São Paulo (FAPESP) and the Research Executive Agency (program COSCALI, No. PIRSES-GA-2010- 268717). C.S., C.Z and S.S acknowledge support by the Deutsche Forschungsgemeinschaft.

[1] S. Inouye, *et al.*, Science **285**, 571 (1999).
[2] R. Bonifacio and L. De Salvo, Nucl. Instrum. Methods A **341**, 360 (1994).
[3] D. Kruse, Ch. von Cube, C. Zimmermann, and Ph.W. Courteille, Phys. Rev. Lett. **91**, 183601 (2003).
[4] S. Slama *et al.*, Phys. Rev. Lett. **98**, 053603 (2007).
[5] N. Piovella, R. Bonifacio, B.W.J. McNeil, and G.R.M. Robb, Opt. Commun.**187**, 165 (1997).
[6] N. Piovella, M. Gatelli, and R. Bonifacio, Opt. Commun. **194**, 167 (2001).
[7] W. Ketterle and Shin Inouye, C. R. Acad. Sci., Ser. IIb **2**, 339 (2001) and cond-mat/0101424.
[8] M. Kozuma et al., Science **286**, 2309 (1999).
[9] T. Bienaimé, *et al.*, Phys. Rev. Lett. **104**, 183602 (2010).
[10] H. Bender, *et al.*, Phys. Rev. A **82**, 011404(R) (2010).
[11] S. Bux, Ch. Gnahm, R.A. Maier, C. Zimmermann, Ph.W. Courteille, Phys. Rev. Lett. **106**, 203601 (2011).
[12] S. Bux, H. Tomczyk, D. Schmidt, N. Piovella, C. Zimmermann, Ph.W. Courteille, New J. Phys., submitted (2012).
[13] W. Ketterle, Phys. Rev. Lett. **106**, 118901 (2010).
[14] Ph.W. Courteille, S. Bux, E. Lucioni, K. Lauber, T. Bienaimé, R. Kaiser, and N. Piovella, Eur. Phys. J. D **58**, 69 (2010).
[15] S. Bux, *et al.*, J. Mod. Opt. **57**, 1841 (2010).
[16] R. Bachelard, N. Piovella, Ph.W. Courteille, Phys. Rev. A **84**, 013821 (2011).
[17] R. Bachelard, Ph.W. Courteille, R. Kaiser, N. Piovella, Europhys. Lett. **97**, 14004 (2012).
[18] T. Bienaimé, M. Petruzzo, D. Bigerni, N. Piovella, R. Kaiser, J. of Mod. Opt. **58**, 1942 (2011).
[19] A.A. Svidzinsky, J.-T. Chang, and M.O. Scully, Phys. Rev. A **81**, 053821 (2010).
[20] G. Mie, Ann. Phys. **330**, 377 (1908), "Beiträge zur Optik trüber Medien, speziell kolloidaler Metallösungen".
[21] C.F. Bohren and D.R. Huffman, *Absorption and Scattering of Light from Small Particles*, Wiley, (1998).
[22] G.K. Campbell, *et al.*, Phys. Rev. Lett. **94**, 170403 (2005).
[23] M.O. Scully, E.S. Fry, C.H. Raymond Ooi, and K. Wdkiewicz, Phys. Rev. Lett. **96**, 010501 (2006).
[24] T. Bienaimé, N. Piovella and R. Kaiser, Phys. Rev. Lett. **108**, 123602 (2012).
[25] The single-atom spontaneous decay term $-(\Gamma/2)\beta$ in Eq.(8) arises from the non-commutation properties of the bosonic operators $\hat{\Psi}_g$ and $\hat{\Psi}_e$, analogously to the spontaneous emission from vacuum arising from the commutation rule for $\hat{a}_\mathbf{k}$. The single-atom decay term, however, is negligible far from the atomic transition ($\Delta_0 \gg \Gamma$), as

will be assumed in the present work.